Yonsei Medical Journal
Vol. 44, No. 2, pp. 249 - 258, 2003

Evaluation of the Post-Shunt Status with Electron Beam Computed Tomography in Cyanotic Congenital Heart Disease

Byoung Wook Choi[1], Young Hwan Park[2], Jong Kyun Lee[3], Min Jung Kim[1], Dong Joon Kim[1], Seok Jong Ryu[1], Bum Koo Cho[2], and Kyu Ok Choe[1]

[1]Department of Diagnostic Radiology and Research Institute of Radiological Science, Divisions of [2]Cardiovascular Surgery and [3]Pediatric Cardiology of Yonsei Cardiovascular Center, Yonsei University College of Medicine, Seoul, Korea.

The assessment of the accuracy of Electron Beam Computed Tomography (EBCT) for the follow-up of pulmonary vascular system after the shunt operation in cyanotic congenital heart diseases was purpose of the study. The study group consists of 16 consecutive patients with cyanotic congenital heart disease who had Blalock-Taussig (BT) shunt (n=7), bi-directional cavo-pulmonary shunt (BCPS, n=7) and unifocalization (n=2). EBT images were obtained on systolic phase under EKG gating and after intravenous administration of contrast agent. We evaluated the shunt patency, anatomy of intrapericardial pulmonary artery, parenchymal pulmonary vessels and background lung attenuation for the pulmonary blood flow, and the presence of systemic arterial and venous collaterals. Angiography (n=12) and echocardiography (n=16) were used as the gold standards. EBCT was consistent with angiogram in detecting the shunt patency and in depicting the anatomy of the intrapericardial pulmonary artery. Occlusion of the BT shunts was not detected in 2 patients by echocardiography. Diffuse or focally decreased pulmonary flow on EBCT in 8 patients was consistent with the pulmonary hemodynamics pattern revealed by cardiac catheterization. Uneven attenuation between lobes was related with multifocal supply of pulmonary flow or occlusion of lobar pulmonary arteries. Systemic collateral arteries were observed in 5 at the corresponding site of the decreased pulmonary flow. Systemic venous collaterals seen in all patients following BCPS were eventually draining to the inferior vena cava in 5 and to the left atrium in 2. EBCT provided accurate information of the pulmonary vascular system after shunt and has unique advantage over echocardiography in assessing patency of BT shunt or unifocalization tubes within the pleural space, the estimation of regional difference in pulmonary hemodynamics, and the detection of systemic collateral vessels. Therefore EBCT may provide useful information about the timing of definitive correction and the need for a second shunt or an interventional procedure prior to total repair.

Key Words: Heart, congenital abnormalities; heart, EBCT; shunt, systemic-pulmonary

Received June 19, 2002
Accepted November 5, 2002

Reprint address: requests to Dr. Kyu Ok Choe, Department of Diagnostic Radiology, Yonsei University College of Medicine, 134 Shinchon-dong, Seodaemun-gu, Seoul 120-752, Korea. Tel: 82-2-361-5834, Fax: 82-2-393-3035, E-mail: kochoe@yumc.yonsei.ac.kr

INTRODUCTION

In many forms of congenital heart disease (CHD) with decreased pulmonary blood flow (PBF), definitive repair is often delayed because of inadequate anatomy of the pulmonary artery (PA).[1,2] Palliative surgery such as modified Blalock-Taussig (BT) shunt, central shunt in case of hypoplasia of central PA, unifocalization procedure in case of pulmonary atresia with multifocal supply of PBF or bi-directional cavo-pulmonary shunt (BCPS) in a single ventricle, which are designed to increase PBF and help develop the pulmonary vascular system, are offered. Following such shunts, information about the anatomic and hemodynamic changes in the pulmonary vasculature is important in timing the subsequent definitive repair or in deciding on the need for any additional shunt procedures to further increase the PBF.[1] Cardiac catheterization and echocardiography have been used for these purposes.[1,3]

Cardiac catheterization, in conjunction with selective angiography, is capable of providing

detailed and accurate information on cardiac defects, the pulmonary hemodynamics, and the major aorto-pulmonary collateral arteries (MAPCA), which are often seen in these cyanotic patients. It is, however, invasive and is not amenable for repeated use in small, sick children.[4] Echocardiography, a non-invasive method, is excellent for evaluating the anatomy and function of the heart.[3] However, because of its small acoustic window its usefulness is limited in the study of the parenchymal PAs.[5] Its use is also difficult during the post-operative period because of scars, surgical wires and synthetic materials which may cause echo reflections.[6]

Electron beam computed tomography (EBCT), an imaging modality with high temporal resolution,[7] is non-invasive diagnostic modality which needs no or only light sedation, making it an excellent examining tool that can be used safely, especially in critically-ill children.[8,9] CT has the additional advantage of being able to visualize the pulmonary vessels,[10,11] the background lung attenuation,[11-13] and the systemic collateral arteries[14,15] and veins[16] in the mediastinum and chest wall.

In this series, we utilized EBCT in 16 patients who had various types of shunt surgery, in order to evaluate the patency of their shunts, the anatomy of the central and peripheral pulmonary vessels and the presence or absence of collateral vessels in the mediastinum and the chest wall. The findings on EBCT were compared to those obtained by cardiac catheterization and echocardiography to determine the relative accuracy and usefulness of EBCT.

MATERIALS AND METHODS

Sixteen consecutive patients with cyanotic CHD who underwent palliative shunt procedures and had EBCT examinations were included in this study. There were 11 boys and 5 girls with ages ranging from 3 months to 12 years (mean 3.8 years). The cardiac defects, which required shunt operation, are listed in Table 1 with the common denominators being pulmonary atresia or pulmo-

Table 1. The Basic Cardiac Defects of Patients and the Type of Shunt Performed

Case No	Shunt type	Basic cardiac defects
1	BT shunt	DORV with VSD, PS, LPA interruption
2	BT shunt	LI, AVSD with unbalanced ventricles, pulmonary atresia
3	BT shunt	TOF
4-6	BT shunt	Pulmonary atresia with VSD
7	BT shunt	Pulmonary atresia with VSD, MAPCA
8	Unifocalization	RI, SV, PS, with MAPCA
9	Unifocalization	RI, AVSD, pulmonary atresia, with MAPCA
10	BCPS	LI, SV, PS
11	BCPS	TA, pulmonary atresia, VSD, post-shunt LPA occlusion
12	BCPS	AVSD with unbalanced ventricles, PS
13	BCPS	LI, SV, pulmonary atresia
14	BCPS	RI, TAPVR, AVSD, pulmonary atresia
15	BCPS	Pulmonary atresia with IVS
16	BCPS	RI, TAPVR, AVSD, PS

AVSD, Atrioventricular septal defect; BCPS, bidirectional cavo-pulmonary shunt; BT, Blalock-Taussig; DORV, Double outlet right ventricle; IVS, Intact ventricular septum; LI, Left isomerism; LPA, Left pulmonary artery; MAPCA, Major aortopulmonary collateral artery; RI, Right isomerism; PS, Pulmonary stenosis; SV, Single ventricle; TAPVR, Total anomalous pulmonary venous return; TA, Tricuspid atresia; TOF, Tetraloy of Fallot; VSD, Ventricular septal defect.

nary stenosis (PS) in all cases. Eight BT shunts were performed in 7 patients, unilateral unifocalization procedures in 2 patients and BCPS in 7 patients. The BCPS was done unilaterally in 4 and bilaterally in 3, thus total 10 superior vena cava-PA shunts were performed. EBCT was performed between 6 days and 2 years after surgery. Twelve patients had both cardiac catheterization and echocardiography and 4 patients had echocardiography only.

EBCT (IMATRON C-150, San Francisco, CA, USA) images were obtained from the diaphragm to the thoracic inlet using a single slice mode at the end-systolic (40% of R-R interval) and the diastasis (80% of R-R interval) phases. The scan time was 100 msec and the slice thickness 3 mm. Contrast agent (Optiray 320, Mallinkrodt Medical Inc. St. Louis, MO, USA) was injected intravenously (2 ml/kg) at the rate of 0.2 - 0.3 ml/sec. Images were obtained 10 seconds after initiation of the injection under quiet breathing and each series required about 15 seconds.

The following four aspects were evaluated. 1) The patency of shunts defined as either homogenous enhancement of the inner lumen of the m-BT shunt, unifocalization tube or anastomosed SVC. 2) The anatomy of the intra-pericardial PA. The diameter of the PA was measured in the systolic images, in which PAs were larger than in the diastolic images. These were measured at multiple levels; main PA at its widest point between the pulmonary valve and the bifurcation, the right PA just before the branching of the anterior truncus and the left PA before the take off of the left upper lobe branch (Fig. 1B), according to the method of Blackstone et al.[17] The shortest axis diameter was measured to compensate for the obliquity of the vessels. The measurement was obtained in the mediastinal window (the level, 80 - 100 HU and width, 550 - 600 HU) in all patients. The confluence of the right and left PAs (Fig. 2A) and the presence of congenital or post-shunt peripheral PS (Fig. 1B) were also evaluated. The degree of stenosis was expressed as the percentage decrease from the maximum diameter of the right and left PAs. 3) The intraparenchymal pulmonary vessels and background attenuation of the lung parenchyma were evaluated to estimate the local PBF by visual inspection. If both intraparenchmal PAs and pulmonary veins were attenuated and the background attenuation decreased, it was assumed to indicate decreased PBF (Fig. 1C and 3B).[10] The reverse was true for increased PBF. Diffuse ground glass opacity of the lung parenchyma associated with peribronchial cuffing, interlobular septal thickening and pleural effusion was classified as pulmonary venous congestion. 4) The development of systemic arterial and venous collaterals was evaluated. The draining sites of the collateral veins were examined. A dilated bronchial artery was defined as vessels around the major airways in the mediastinum on the contrast-enhanced EBCT studies (Fig. 2A). The internal mammary artery was considered to be dilated when its diameter was greater than that on the opposite side (Fig. 2A). Transpleural collateral arteries via arteries of the chest wall were defined as the presence of numerous linear opacities perpendicular to the pleura[15] (Fig. 2D) accompanied by dilatation of the intercostal or internal mammary arteries. Collateral systemic veins were observed in some post-BCPS patients. The venous collaterals tended to be more serpentine in course, larger than the systemic collateral arteries and mostly located in the posterior paravertebral areas (Fig. 4A-C), while the collateral arteries were usually seen along the upper chest wall.

All the above findings were evaluated by 2 board-certified thoracic radiologists, who were blinded to the angiographic results. The EBCT findings were compared with the results obtained by cardiac catheterization and echocardiography.

RESULTS

The patency of the shunt

Of the 20 shunts (16 patients) seen on EBCT examinations, 18 shunts were judged to be patent and 2 BT shunts occluded (Fig. 1A). Shunt patency observed on EBCT was consistent with the results of the catheterized patients (Fig. 2 - 4). Echocardiography was correct in revealing the patency of BCPS but was not able to detect the BT shunt grafts or unifocalization tubes, which were within

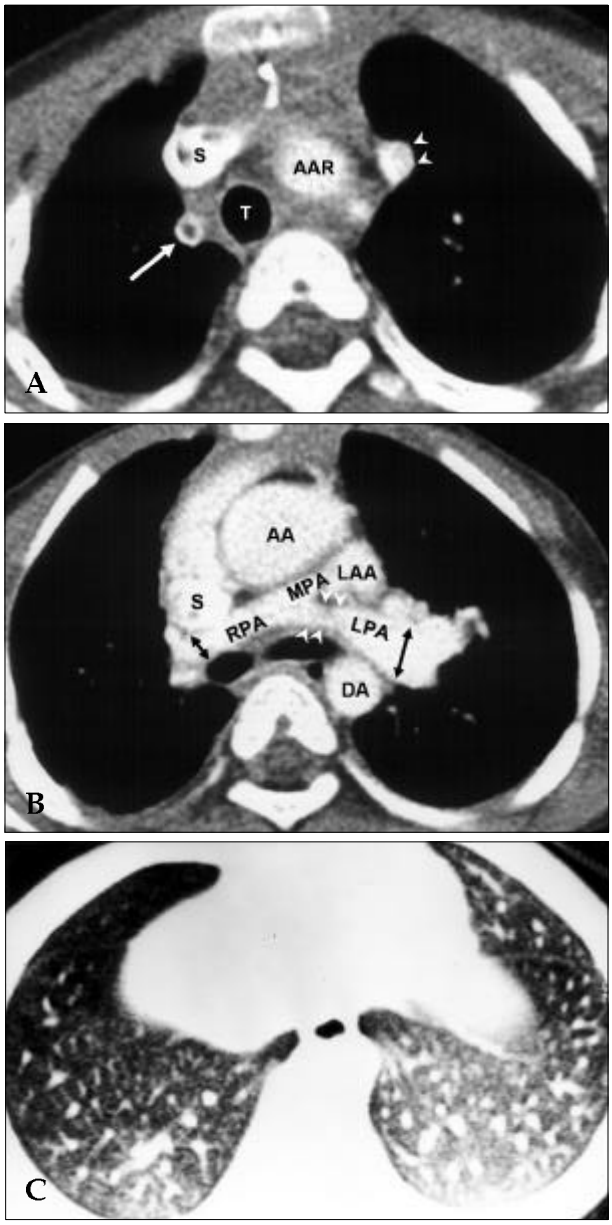

Fig. 1. A 5-month-old girl (case 4) with pulmonary atresia with VSD and a junctional stenosis of the left pulmonary artery (LPA), for which bilateral modified BT shunts was performed. A) EBT slice just above the aortic arch (AAR). The lumen of the right modified BT shunt (white arrow) does not enhance at all after intravenous contrast administration, while the left modified BT shunt (white arrowheads) becomes densely enhanced, suggestive of occluded right, but patent left shunt. The right BT shunt wall, composed of PTFE (polytetrafluoroethylene), is highly attenuated. B) 24mm caudad to the slice A. Although MPA is hypoplastic, the right and left pulmonary arteries are confluent to each other. A juxta-ductal stenosis (white arrowheads) is noted at the proximal LPA. The distal and hilar LPA is dilated because of the preferential blood flow to the LPA via the patent left BT shunt, while blood flow to the right is limited by juxta-ductal stenosis and the occluded right BT shunt. The diameter of the right PA was measured just before the branching of the anterior truncus (right bi-directional arrow) and the left PA before the take off of the left upper lobe branch (left bi-directional arrow). C) The lower lung field in lung window setting reveals diffuse attenuation of the pulmonary vessels and diffuse decrease in lung attenuation on the right, due to an asymmetric decrease of the pulmonary blood flow. As the flow through the shunt preferentially supplies the left lung, the pulmonary blood flow to the right becomes decreased. AA, ascending aorta; AAR, aortic arch; DA, descending aorta; LAA, left atrial appendage; LPA, left pulmonary artery; MPA, main pulmonary artery; RPA, right pulmonary artery; S, superior vena cava; T, trachea.

the pleural space, and therefore failed to demonstrate the graft occlusion of the 2 BT shunts.

Size, confluence and stenosis of PA

The size of the main, left and right PAs measured on EBCT were compared with those obtained by catheterization. The data obtained at cardiac catheterization and EBCT showed a high linear correlation (r=0.91, $p<0.01$) in the 12 catheterized patients. EBCT identified the confluence of the PAs in 14 patients, interruption or post-shunt occlusion of the PA in 2 patients (Fig. 2A). EBT revealed significant (> 50%) juxtaductal PS (Fig. 1B) in 2 patients and post-shunt PS in another. Cardiac catheterization confirmed compatible findings in all 12 patients. There was no instance of greater than 50% PS found on cardiac catheterization or echocardiography, but missed by EBCT. In the patient with interruption/occlusion of the PA, the length of the obliterated segment as well as the size of the hilar PA distal to the interruption/occlusion (Fig. 2A) could be measured on EBCT (Fig. 2B).

Evaluation of the parenchymal pulmonary flow

The intraparenchymal pulmonary vessels and the background lung attenuation assessed by EBCT were normal in 6 patients (Fig. 4E), decreased symmetrically in 1, asymmetrically in 2 (Fig. 1C and 2D), and unevenly between the lobes in 5 (Fig. 3B). In 2 patients pulmonary venous congestion was present (Table 2). In 5 of 6 cases with normal pulmonary vascularity, both EBCT and catheterization showed a patent shunt, normal-sized central PA, absence of peripheral PS and homogeneous lung attenuation or capillary blush. In the remaining one after BCPS, although the lung attenuation and peripheral pulmonary vasculature were normal, there was a mild hypoplasia of the central PA on EBCT and cardiac catheterization.

In the patient with symmetrical and even decrease of PBF, EBCT and catheterization revealed patent shunt but diffuse hypoplasia of central PA. Two patients with asymmetric decrease in the right lung attenuation (Fig. 1 and 2) had either juxta- ductal stenosis (Fig. 1C) or interruption of left PA (Fig. 2A). Angiography confirmed the findings that the patent left BT shunt preferentially or only supplied blood into the left lung beyond stenosis or interruption (Fig. 2B).

Uneven attenuation between the lobes was observed on EBCT in 5 patients. Three of the 5 patients the lungs received multifocal blood supply from MAPCA. Unilateral unifocalization procedure that had been performed in 2 was found to be patent on EBT. The unoperated lung still demonstrated uneven lobar density from persistent multifocal blood supply via MAPCA on cardiac angiography (Fig. 3C). Of the remaining 2 patients, decreased attenuation of a lobe was confirmed in 1 by angiography to be occlusion of right middle lobar PAs next to the previous BT or BCPS shunt sites. The occlusion was suggestive of post-shunt complication. EBCT did not identify individual MAPCA or verify the occlusion of lobar PAs in the above 5 patients, because of their small diameter.

Bilateral or unilateral pulmonary venous congestion was noted in 2 cases. The patient with bilateral venous congestion had undergone a BT shunt for tetralogy of Fallot and later developed dilated cardiomyopathy. The other patient with unilateral venous congestion on EBCT had a BCPS and a repair of total anomalous pulmonary venous return of the supracardiac type. Stenosis of the right pulmonary vein was found on EBCT and this was confirmed by angiography.

Systemic arterial and venous collaterals

Development of systemic collateral arteries was seen in 5 of the 8 cases who showed symmetric (n=1), asymmetric (n=2) or lobar (n=2) decrease in attenuation of the lungs. Their location coincided

Table 2. The Peripheral Pulmonary Vasculature on EBCT and the Anatomy of Central Pulmonary Arteries on Catheterization and/or Echocardiography

Peripheral vascularity on EBT	Anatomy of Central PA & Origin Supply of PBF by Catheterization/ Echocardiography
Normal (n=6)	Patent shunt, absence of peripheral PS, normal growth (cases 5,6,10,12,15) or slight hypoplasia of central PA (case 13)
Symmetric decrease (n=1)	hypoplastic central PA (case 2)
Asymmetric decrease (n=2)	Left PA stenosis (case 4), Left PA interruption (case 1)
Uneven attenuation between lobes (n=5)	Multifocal supply from MAPCA (cases 7,8,9) Post-shunt occlusion of lobar PA (cases 11,14)
PV congestion (n=2)	TOF with dilated CMP (case 3) PV stenosis after repair of TAPVR (case 16)

PA, pulmonary artery; PBF, pulmonary blood flow; PS, pulmonary stenosis; PV, pulmonary vein; MAPCA, major aortopulmonary collateral artery; TOF, tetralogy of Fallot; CMP, cardiomyopathy; TAPVR, total anomalous pulmonary venous return.

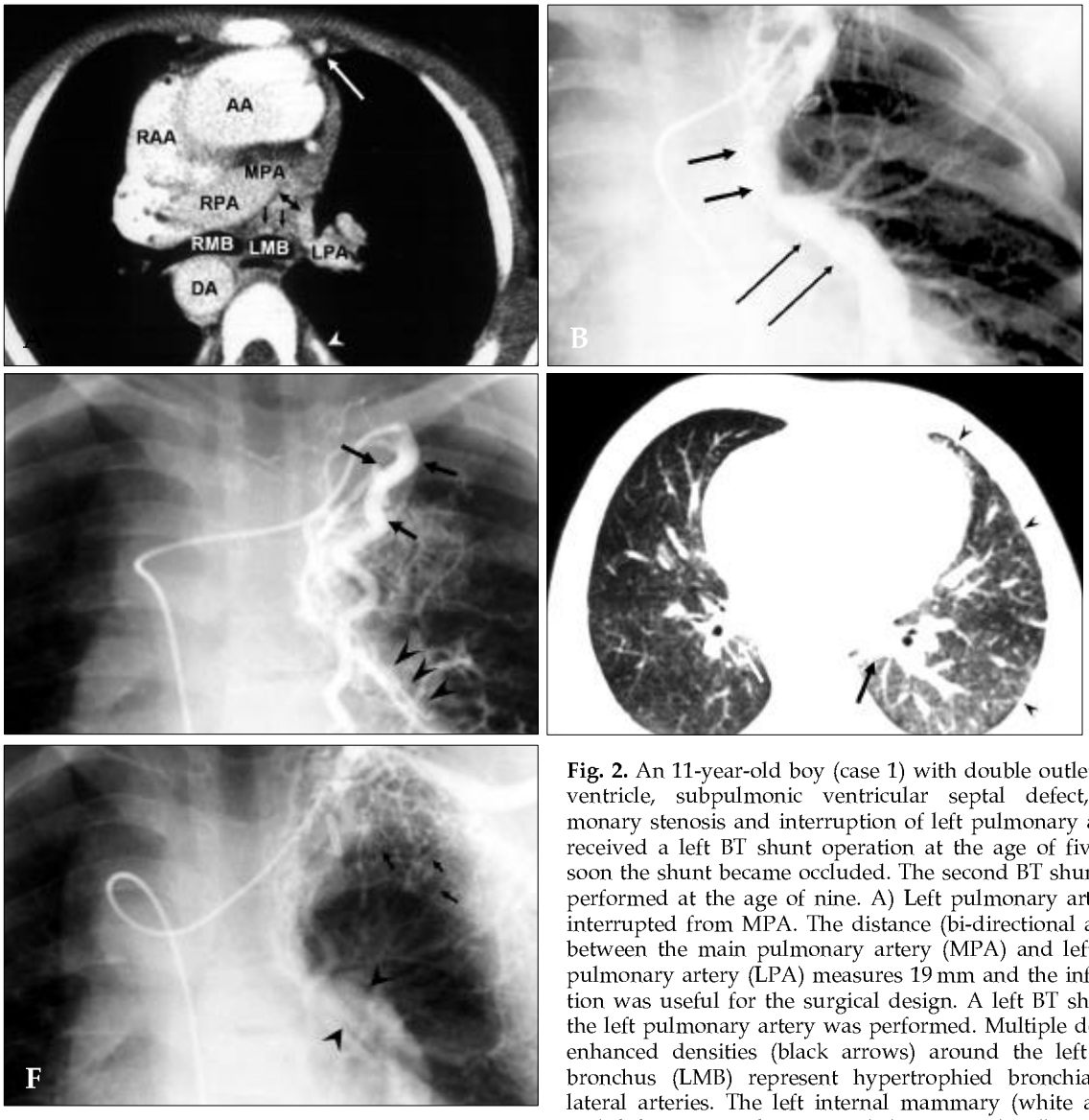

Fig. 2. An 11-year-old boy (case 1) with double outlet right ventricle, subpulmonic ventricular septal defect, pulmonary stenosis and interruption of left pulmonary artery, received a left BT shunt operation at the age of five, but soon the shunt became occluded. The second BT shunt was performed at the age of nine. A) Left pulmonary artery is interrupted from MPA. The distance (bi-directional arrow) between the main pulmonary artery (MPA) and left hilar pulmonary artery (LPA) measures 19 mm and the information was useful for the surgical design. A left BT shunt to the left pulmonary artery was performed. Multiple dot-like enhanced densities (black arrows) around the left main bronchus (LMB) represent hypertrophied bronchial collateral arteries. The left internal mammary (white arrow) and left intercostal arteries (white arrowhead) are also hypertrophied. B) The selective angiogram of the left BT shunt (thick arrows) supplies only the left pulmonary artery (thin arrow), however, the gap between the main and left pulmonary arteries cannot be measured by this projectional image. PBF to the right lung was only supplied from the right ventricle and was decreased due to tight pulmonary stenosis. C) On selective angiogram of the left internal mammary artery (arrows), the vessels correspond to hypertrophied bronchial collateral arteries coursing along the wall of the left main and lower lobar bronchi (arrowheads). This systemic arterial collateral persists probably because of occlusive complication of the first BT shunt and pleural adhesion after two BT shunt procedures. A total cavopulmonary connection was performed 2 years after this study and embolization of the systemic collateral had been done just before the definitive palliative repair. D) The right lung in the lung window setting reveals diffusely attenuated pulmonary vessels and decreased lung attenuation compared to the left. The right inferior pulmonary vein (white arrow) is smaller than the left inferior pulmonary vein (black arrow) and it is another sign of decreased pulmonary blood flow to the right lung. Numerous band-like densities at the subpleural area of the left lung (arrowheads) were compatible with transpleural collateral formation from the systemic arteries of the chest wall. E) On the late phase of selective angiogram of the left lateral thoracic artery (thick arrows), numerous transpleural collateral arteries are communicating with the subpleural pulmonary arterioles (thin arrows), which are retrogradely opacifying the perihilar pulmonary arterial branches (arrowheads). The subpleural linear densities observed by CT are suggestive of transpleural collateral arteries originating from intercostal arteries, anastomosed with small peripheral pulmonary arterial branches beyond the interruption. AA, ascending aorta; BT, Blalock Taussing; DA, descending aorta; DORV, Double outlet right ventricle; LMB, left main bronchus; LPA, left hilar pulmonary artery; RAA, right atrial appendage; RMB, right main

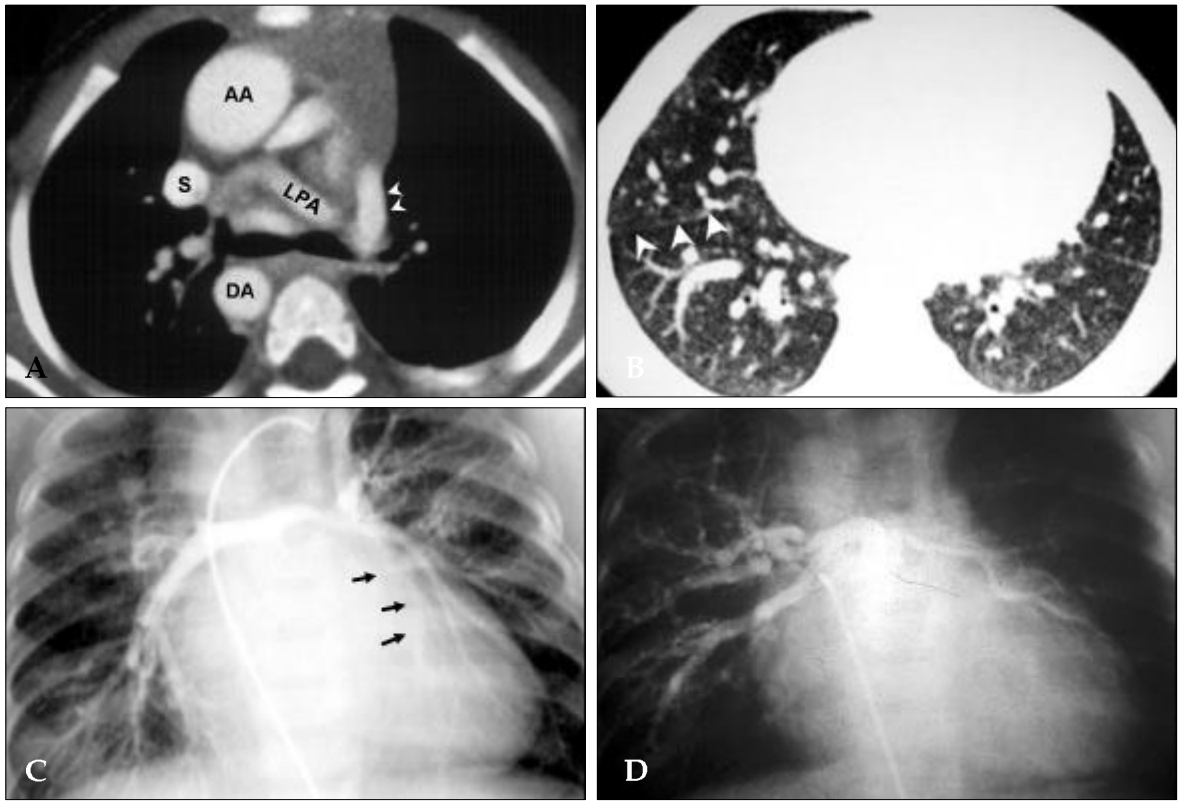

Fig. 3. A 1-year-old boy (case 9) with right isomerism, atrioventricular septal defect, pulmonary atresia with multifocal pulmonary arterial supply by the major aortopulmonary collateral arteries. Unifocalization procedure has been performed only on the left side. A) Homogeneous contrast enhancement of the left BT (white arrowheads) suggests its patency. Left pulmonary artery is still hypoplastic. B) Uneven attenuation between lobes is noted. The lung attenuation of the right middle lobe is lower than that of right lower lobe. The peripheral pulmonary vasculature shows dilation of perihilar vessels but paucity of side branches in the right middle lobe, compared to the vessels in right lower lobe. The right major fissure is indicated with arrowheads. C) The angiogram from the left BT shunt revealed the central PA, left upper lobar and right lower lobar PA branches. The left lower lobar pulmonary artery (black arrows) is faintly opacified because of competitive flow from the major aortopulmonary collateral artery, which is still patent. Mean pressure of left PA is 15 mmHg. The branches of right lower lobe show regular branching and tapering, and abundant side branches. D) The selective angiogram of a MAPCA, supplying the right upper and middle lobar pulmonary arteries, revealed dilated tortuous branches with paucity of small side branches and decreased capillary blush. This findings are contrary to the vessels in the right lower lobe in Fig 3C. AA, ascending aorta; BT, Blalock Taussing; DA, descending aorta; LPA, left pulmonary artery; S, superior vena cava.

with site of the previous palliative shunt operation and pleural adhesion (Fig. 2A and D). Angiography (n=4) revealed these vessels arising from the intercostal, bronchial, internal thoracic and subclavian arteries (Fig. 2C and E). Systemic venous collaterals were identified on EBCT in all 7 patients who had undergone BCPS (Fig. 4A-C). Using EBCT, it was possible to trace the drainage sites in all patients, 5 into the azygous, hemiazygous and lumbar veins and 2 directly into the left atrium. Angiography performed in 2 cases confirmed the findings by EBCT (Fig. 4D).

DISCUSSION

In managing the patients with CHD with decreased PBF and shunt procedures, the post-shunt size and anatomy of the PA is critical in detecting complications related to shunting and in determining the need and timing of subsequent surgery.[18-20] In the study of congenital cardiac defects, the current trend is to use echocardiography first for routine study and to reserve cardiac catheterization only for the patients who may require specific hemodynamic information or therapeutic intervention.[21] Echocardiography was excellent in evaluating the shunt and PA status

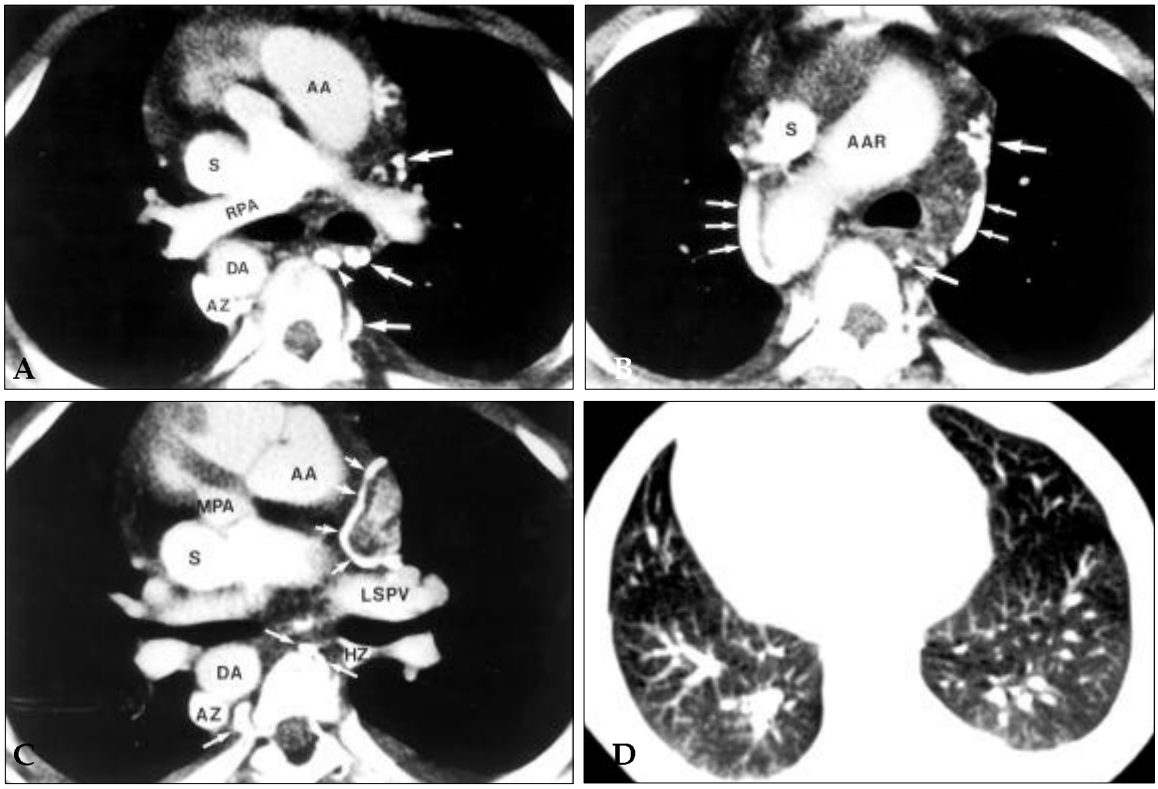

Fig. 4. A 12-year-old boy (case 10) with left isomerism, single ventricle with pulmonary stenosis. Right BCPS was performed. A-B) Right superior vena cava (S) anastomosed with right pulmonary artery (RPA). Multiple enhancing vascular structures are found in the mediastinum. The veins in B are the right and left superior intercostal veins (small white arrows). The veins in A are the markedly-dilated right azygous vein (Az) and the dilated hemiazygous (white arrowhead) and paravertebral venous plexus or other mediastinal veins (large white arrows). These veins are larger-bored and less numerous than the systemic collateral arteries (compare with Fig. 2A). C) In the pericardial space, a heterogeneously enhancing lesion with outer ring-like calcification (short arrows) is noted anterior to the left superior pulmonary vein (LSPV). A necrotic mediastinal abscess was diagnosed and drained by the operation. Dilated azygous (AZ), hemiazygous (HZ), and multiple mediastinal veins (long arrows) are also seen. D) Evenly-tapered and normal-sized pulmonary vascular branches and homogeneous background attenuation are seen in bilateral lung parenchyma in HRCT. AA, Ascending aorta; AAR, aortic arch; AZ, azygous vein; BCPS, Bidirectional cavopulmonary shunt; DA, Descending aorta; HZ, hemoazygous vein; LSPV, left superior pulmonary vein; RPA, right pulmonary artery; S, Superior vena cava.

within the pericardium in our study, such as the patency of BCPS, development of central PA or detection of peripheral PS. But echocardiographic use was limited outside the pericardium.[5,6] EBCT was superior to echocardiography in evaluating the patency of BT shunts or unifocalization tubes located within the pleural cavity. Also EBCT was able to measure the size of the hilar PA distal to the interruption and the length of the interrupted/obliterated segment, while angiography and echocardiography cannot always detect the vessel segment distal to the occlusion.

Another advantage of EBCT was estimating regional differences in pulmonary hemodynamics by assessing the peripheral pulmonary vessels and the background lung density.[10-13] The background density of lung observed with EBCT may correspond to the parenchymal blush in the capillary phase of pulmonary angiogram.[22,23] Most frequently observed pattern of pulmonary vasculature was decrease of PBF in this particular patient group. Symmetric or asymmetric decrease of lung attenuation in EBCT were all consistent with the restriction of PBF to one or both lungs subsequent to shunt occlusion and/or deformity of the central PAs revealed by cardiac catheterization. The uneven lobar attenuation seen on EBCT was closely related with heterogeneity of regional PBF due either to multifocal origin of the PBF or to post-shunt occlusion of a lobar PA in

our study. In pulmonary atresia with complicated arborization anomalies of PA, total correction is contraindicated, unless the continuity between right ventricle and more than 10 segmental PAs with normal pulmonary vascular resistance can be established.[24] Angiography may be limited to provide quantitative regional pulmonary hemodynamics in such situation because of difficulty in selecting every PA branches distal to stenotic PA or MAPCA.[19] Lung perfusion scan using radioisotope may be another option to confirm the heterogeneous PBF but this technique is in general not recommended in CHD with right to left shunt. However, EBCT may have a role in inferring the regional difference of PBF in this disease subset, which needs further investigation.

In addition, high spatial resolution of EBCT allows the detection of systemic collateral arteries and veins in contrast-enhanced images.[14-16] Development of systemic collateral arteries can be a major problem during cardiopulmonary bypass, causing insufficient perfusion of the major organs and inadequate protection of myocardium due to an increase in pulmonary arterial flow and venous return.[25] The presence of the systemic arterial collaterals is a bad prognostic sign after total cavopulmonary connection (TCPC), as it elevates the pulmonary vascular resistance and competes with the flow through the low-pressure vena cavi.[26,27] Systemic venous collateral flow was reported to develop in about one-third of patients following BCPS by angiography[28] but they were found in all of the patients with BCPS in this study, suggesting higher incidence of venous collateral than expected. There are two types of the drainage pathways: SVC to inferior vena caval venous connection and SVC to left atrium or pulmonary venous connection. The collateral flow into the subdiaphragmatic systemic veins and inferior vena cava is not important clinically as it disappears after TCPC, except in the cases with interruption of inferior vena cava. However it is important to know the presence of collateral veins draining into the pulmonary vein and left atrium, because these collaterals do not disappear spontaneously and cause systemic arterial desaturation after TCPC,[29] therefore they must be obliterated before or at the time of TCPC. Echocardiography was limited in visualization of collateral vessels usually in far posterior mediastinum.

The EBCT images could not be obtained under suspension of breath in small children. However, the pulmonary vascularity was most frequently normal or regionally decreased in this disease subset. EBCT does not provide sufficient functional hemodynamic information because of temporal resolution. Pulmonary blood volume manifests as an increase in lung density and a dilatation of pulmonary vessels, and PBF is a combination of pulmonary blood volume and transit time.[30] Recent advances in CT technology may allow the measurement of circulation time with administration of contrast media, thus CT can objectively quantitate the absolute value of regional PBF. Combined echocardiography provides hemodynamic data, particularly of ventricular and valve function. The spatial resolution of EBCT was not high enough to detect MAPCAs or occluded lobar PAs and was able to detect stenosis of the intrapericardial and hilar PAs.

In conclusion, EBCT proved to be a valuable imaging tool in the follow-up of patients with various types of shunts. It can provide information about patency of the shunts, anatomy of the central PAs, the peripheral pulmonary vascularity and the development of systemic collateral vessels. EBCT has unique advantage over echocardiography in assessing patency of BT shunt or unifocalization tubes within the pleural space, the estimation of regional difference in pulmonary vasculature, the detection of systemic collateral vessels including veins directly draining to systemic cardiac chambers. Thereby EBCT may provide valuable information about the timing of total repair and the need for a second shunt or a catheterized procedures prior to total repair.

REFERENCES

1. Zellner JL, Sade RM. Palliative procedures in cyanotic congenital heart disease. In: Baue AE, Geha AS, Hammond GL, Laks H, Naunheim KS, Editors. Glenn's Thoracic and Cardiovascular Surgery. 6th ed. Stanford, Conn.: Appleton & Lange; 1996. p.1073-81.
2. Pridjian AK, Mendelsohn AM, Lupinetti FM, Beekmen RH 3rd, Dick M 2nd, Serwer G, et al,. Usefulness of the bidirectional Glenn procedure as staged reconstruction for the functional single ventricle. Am J Cardiol 1993; 71:959-62.

3. Grossman W. Complications of cardiac catheterization: incidence, cause, and prevention. In: Grossman W, Baim DB, Editors. Cardiac catheterization and intervention. 4th ed. Philadelphia: Lea & Febiger; 1991. p.28-43.
4. Child JS. Echo-Doppler and color-flow imaging in congenital heart disease. Cardiol Clin 1990;8:289-313.
5. Duerinckx AJ, Wexler L, Banerjee A, Higgins SS, Hardy CE, Helton G, et al. Postoperative evaluation of pulmonary arteries in congenital heart surgery by magnetic resonance imaging: comparison with echocardiography. Am Heart J 1994;128:1139-46.
6. Borneimer R, Weinberg PM, Fogel MA. Angiographic, echocardiographic, and three-dimensional magnetic resonance imaging of extracardiac conduits in congenital heart disease. Am J Cardiol 1996;78:713-7.
7. Gould RG. Principles of ultrafast computed tomography: historical aspects, mechanism of action, and scanner characteristics. In: Stanford W, Rumberger JA, editors. Ultrafast computed tomography in cardiac imaging: principles and practice. New York: Futura; 1992. p.1-15.
8. Husayni TS. Ultrafast computed tomographic imaging in congenital heart disease. In: Stanford W, Rumberger JA, Editors. Ultrafast computed tomography in cardiac imaging: principles and practice. New York: Futura; 1992. p.311-37.
9. Brasch RC. Ultrafast computed tomography for infants and children. Radiol Clin North Am 1988;26:277-86.
10. Choe KO, Hong YK, Kim HJ, Joo SH, Cho BK, Chang BC, et al. The use of high resolution computed tomogrpahy in the evaluation of pulmonary hemodynamics in patients with congenital heart disease. Pediatr Cardiol 2000;21:202-10.
11. Herold CJ, Wetzel RC, Robotham JL, Herold SM, Zerhouni EA. Acute effects of increased intravascular volume and hypoxia on the pulmonary circulation: Assessment with high-resolution CT. Radiology 1992; 183:655-62.
12. Worthy SA, Muller NL, Hartmen TE, Swenson SJ, Padley SP, Hansell DM. Mosaic attenuation pattern on thin section CT scans of the lung: differentiation among infiltrative lung, airway, and vascular disease as a cause. Radiology 1997;205:465-70.
13. Vock P, Salzmann C. Comparison of computed tomographic lung density with hemodynamic data of the pulmonary circulation. Clin Radiol 1986;37:459-64.
14. Kauczor HU, Scheickert HC, Mayer E, Schweden F, Schild HH, Thelen M. Spiral CT of bronchial arteries in chronic thromboembolism. J Comput Assist Tomogr 1994;18:855-61.
15. Ryu DS, Kim NH, Jung SM, Kim JK, Park MS. Transpleural subclavian artery to pulmonary artery anastomosis. J Comput Assist Tomogr 1998;22;922-4.
16. Qanadli SD, Hajjam ME, Bruckert F, Judet O, Barre O, Chagnon S, et al. Helical CT phlebography of the superior vena cava: Diagnosis ad evaluation of venous obstruction. Am J Roentgenol 1998;72:1327-33.
17. Blacksone EH, Kirklin JW, Bertrnou EG, Labrosse CJ, Soto B, Bargeron LM. Preoperative prediction from cineangiograms of post-repair right ventricular pressure in tetralogy of Fallot. J Thorac Cardiovasc Surg 1979;78: 542-52.
18. Godart F, Qureshi SA, Simha A, Deverall PB, Anderson DR, Baker EJ, et al. Effects of modified and classic Blalock-Taussig shunts on the pulmonary arterial tree. Ann Thorac Surg 1998;66:512-7.
19. Ishizaka T, Yagihara T, Yamamoto F, Nishigaki K, Matsuki O, Uemura H, et al. Results of unifocalization for pulmonary atresia, ventricular septal defect and major aortopulmonary collateral arteries: patency of pulmonary vascular segments. Eur J Cardiothorac Surg 1996;10:331-7.
20. Mendelsohn AM, Bove EL, Lupinetti FM, Crowley DC, Lloyd TR, Beekman RH. Central pulmonary artery growth patterns after the bi-directional Glenn procedure. J Thorac Cardiovasc Surg 1994;107:1284-90.
21. Beekman RP, Filipini LH, Meijboom EJ. Evolving usage of pediatric cardiac catheterization. Curr Opin Cardiol 1994;9:721-8.
22. Nihill MR, McNamara DG. Magnification pulmonary wedge angiography in the evaluation of children with congenital heart disease and pulmonary hypertension. Circulation 1978;58:1094-106.
23. Rabinovitch M, Keane JF, Fellows KE, Castaneda AR, Reid L. Quantitative analysis of the pulmonary wedge angiogram in congenital heart defects. Correlation with hemodynamic data and morphometric findings in lung biopsy tissue. Circulation 1981;63:152-64.
24. Kirklin JW, Blackstone EH, Shimazaki Y, Maehara T, Pacifico AD, Kirklin JK, et al. Survival, functional status, and reoperation after repair of tetralogy of Fallot with pulmonary atresia. J Thorac Cardiovasc Surg 1988;96: 102-16.
25. Ataka T, Fukuda S, Kinishita H, Kurokawa S, Kitahara Y, Shimoji K, et al. Anesthetic management of an infant with pulmonary atresia and ventricular septal defect accompanied by excess pulmonary blood flow for systemic-pulmonic shunt operation. Masui 1999;48:372-6.
26. Ichikawa H, Yagihara T, Kishimoto H, Isobe F, Yamamoto F, Nishigaki K, et al. Extent of aorto-pulmonary collateral blood flow as a risk factors for Fontan operations. Ann Thorac Surg 1995;59:433-7.
27. Kanter KR, Vincent RN, Raviele AA. Importance of acquired systemic-to-pulmonary collaterals in the Fontan operation. Ann Thorac Surg 1999;68:969-75.
28. Magee AG, McCrindle BW, Mawson J, Benson LN, Williams WG, Freedom RM. Systemic venous collateral development after the bidirectional cavopulmonary anastomosis. Prevalence and predictors. J Am Coll Cardiol 1998;32:502-8.
29. Gatzoulis MA, Shinebourne EA, Redington AN, Rigby ML, Ho SY, Shore DF. Increasing cyanosis early after cavopulmonary connection caused by abnormal systemic venous channels. Br Heart J 1995;73:182-6.
30. Milne ENC, Pistolesi M. Quantitation of pulmonary blood volume, flow and pressure. Principles and Practices. In: Reading the Chest Radiograph. A Physiologic Approach. St. Louis: Mosby; 1993. p.164-241.